

APPLICATION OF THE 3D CRS WORKFLOW IN CRYSTALLINE ROCK ENVIRONMENT

K. A. Ahmed, D. Gajewski, and B. Schwarz

email: *khawar-ashfaq.ahmed@zmaw.de*

keywords: *3D CRS, Hard rock*

ABSTRACT

Seismic data from crystalline or hard rock environments usually exhibit a poor signal-to-noise (S/N) ratio due to low acoustic impedances in the subsurface. Moreover, instead of continuous reflections we observe a lot of steeply dipping events resembling parts of diffractions. The conventional seismic processing (CMP stack and DMO) is not ideally suited for imaging such type of data. CRS processing considers more traces during the stack than CMP processing and the resulting image displays a better quality. In the last decade, the CRS workflow was established as a powerful tool to provide improved images, especially for low fold or low S/N data. The application of the workflow to the 3D Schneeberg crystalline rock seismic data shows that images of coherence provided the best results for an initial analysis. The CRS stack did not provide an image quality suitable for interpretation. For data from environments with low acoustic impedance the coherence may provide an alternative way to image the subsurface. The analysis of the data has shown that without pre-stack data enhancement methods it may not be possible to generate satisfactory stacked images. Because of the large number of diffractions in the data leading to numerous conflicting dips and crossing image patterns, stacks are difficult to interpret. The first time migration results helped to identify several major fault structures in the data volume which coincide with geological features of the considered area.

INTRODUCTION

3D seismic imaging is a challenge for data acquired in the hard rock environments. The reason for this is the small reflectivity/acoustic impedance and S/N ratio compared to data from sedimentary basins. Contrary to typical reflection data where we observe continuous events of large lateral distances hard rock data are usually dominated by diffractions or parts of diffraction events which leads to a criss-cross pattern and numerous conflicting dip features in the stacked sections. This challenges any kind of interpretation. This makes it difficult to obtain an image of the subsurface structure. The velocity in hard rock is usually high and resulting moveouts are small which provides an additional challenge in the data processing.

Since it was demonstrated previously that the CRS method has advantages for low fold and/or low S/N data when compared with CMP processing, such processing may provide a suitable alternative. It is an important feature that the fold in CRS processing is considerably high that in CMP processing which may help to image weak events. The stacking parameters of the CRS stacking operator are also called kinematic wavefield attributes. The established CRS based work flow usually includes the CRS stacking, automatic picking of the kinematic wave field attributes and NIP wave tomography (Hertweck et al., 2007; Baykulov et al., 2011) and time/depth migration.

In this work we process the 3D Schneeberg seismic reflection data. In a joint project with the University of Freiberg, Freiberg, Germany and Leibniz Institute for Applied Geophysics, Hannover, Germany a 3-D reflection seismic experiment was conducted in the area of the city of Schneeberg, Saxonia, Germany.

The field work is part of a pre-site survey for a geothermal energy project. The subsurface in this area is complex with steep faulting in the crystalline environment. The velocity in this lithology is approximately 6000 m/s. No significant lateral velocity variations are expected within the crystalline rocks. The data show a lot of scattering due to the fractured zones and may be because of hydrothermal veins. The processing of this type of seismic data is a challenge because of the above mentioned reasons. Conventional CMP-DMO-based processing did not provide satisfactory results. Therefore, 3D CRS processing was applied here in the hope to achieve a better S/N ratio and to obtain an interpretable stacked volume.

In a first attempt we will follow a purely data driven approach without considering any prior geological information for processing except the near surface velocity. In this stage coherence is considered. Since these images are difficult to interpret we finally show some time migrated images which represent the current state of the processing.

BASICS OF 3D-CRS BASED WORKFLOW

The CRS stack (Jäger et al., 2001) was originally developed to obtain simulated zero-offset (ZO) sections or volumes from seismic multi-coverage data. The method is based on stacking operators that are of second order in the midpoint and half-offset coordinates x_m and h . The shape of the CRS stacking operator at a given zero-offset location (x_0, t_0) is determined by a number of parameters related to the coefficients of the travel time expansion. For each zero-offset sample to be simulated, the optimum stacking operator is found by varying these parameter values, i.e., the shape of the operator and performing a coherence analysis directly in the pre-stack data. The parameters which yield the highest coherence value describe the optimum stacking operator are called kinematic wavefield attributes. If a locally constant near-surface velocity v_0 is assumed to be known, the CRS operator may be written in the form that allows the interpretation of the kinematic wavefield attributes as parameters describing two hypothetical emerging wave fronts at the considered surface location x_0 . These are the so-called normal-incidence point (NIP) wave and the normal (N) wave (Hubral, 1983). The NIP wave would be observed at x_0 if a point-source were placed at the NIP of the zero-offset ray on a reflector in the subsurface, while the N wave would be obtained if an exploding reflector element -the CRS- were placed around the NIP in the subsurface.

3D-Common-Reflection-Surface Stack

In the 3D case, the emerging wavefronts are locally characterized by their curvatures and their emergence direction at x_0 , which is the same for the NIP and the N wave. If the NIP wave and N wave curvatures are given by 2×2 curvature matrices \mathbf{M}_{nip} and \mathbf{M}_n respectively (each matrix contains three independent elements) and the emergence direction is described by two angles α and β , the 3D CRS operator reads:

$$t^2(\Delta \mathbf{x}_m, h) = (t_0 + \mathbf{p} \Delta \mathbf{x}_m)^2 + 2t_0 \left(\Delta \mathbf{x}_m^T \mathbf{M}_n \Delta \mathbf{x}_m + \mathbf{h}^T \mathbf{M}_{nip} \mathbf{h} \right) \quad (1)$$

It depends on eight stacking parameters: a two component vector \mathbf{p} and two symmetric 2×2 matrices \mathbf{M}_{nip} and \mathbf{M}_n . These stacking parameters represent first and second order travel time derivatives with respect to mid-point and half-offset coordinates. Assuming the near surface velocity v_0 to be known, they may be expressed in terms of kinematic wave field attributes:

$$\mathbf{p}_m = \frac{1}{v_0} (\cos \alpha \sin \beta, \sin \alpha \cos \beta)^T \quad (2)$$

$$\mathbf{M}_{nip} = \frac{1}{v_0} \mathbf{H} \mathbf{K}_{nip} \mathbf{H}^T \quad (3)$$

$$\mathbf{M}_n = \frac{1}{v_0} \mathbf{H} \mathbf{K}_n \mathbf{H}^T \quad (4)$$

where α is azimuth, β is dip angle and \mathbf{H} is the 2×2 upper left sub matrix of the 3×3 transformation matrix from the wavefront coordinate system into the registration surface. These parameters are referred to as the kinematic wavefield attributes. During the 3D CRS stack, along with the simulated ZO section,

a number of volumes containing the optimum kinematic wavefield attributes and coherence for each ZO samples are obtained.

AREA OF STUDY

Schneeberg is a town in the Saxony district of Erzgebirgskreis (Figure 1) located close to the border of Czech Republic. The structure and tectonics of the study area include a massive granitic igneous body overlapping with a number of low, medium and high grade metamorphic rock units. There are also patches of the sedimentary environments in the vicinity of this area.

The origin of the igneous body goes back to an important Cambro-Ordovician phase of rifting, which is detectable almost everywhere in Europe (Emmermann and Wohlenberg, 1988). The alternating metamorphic blocks are layered on that igneous body in a inclined position derived from areas south of the Saxothuringian Zone. This massive igneous body is the prominent feature in this area which has high reflectivity at the transition zone between the metamorphic and igneous rocks and exhibits high velocities in the earth crust.

There is a major steep dipping fault system called Roter Kamm which runs through the igneous body (Figure 2). Some conjugate faulting can be observed in the upper area in NE which runs till the Roter Kamm crossing it perpendicularly and cutting this structure in SW direction. This area is highly fractured with steep dipping tectonics. At the surface the Rote Kamm is characterized by fault systems representing a major structure separating two different types of zones. The dip of the fault and the overlying rocks of the igneous body is towards north-east.

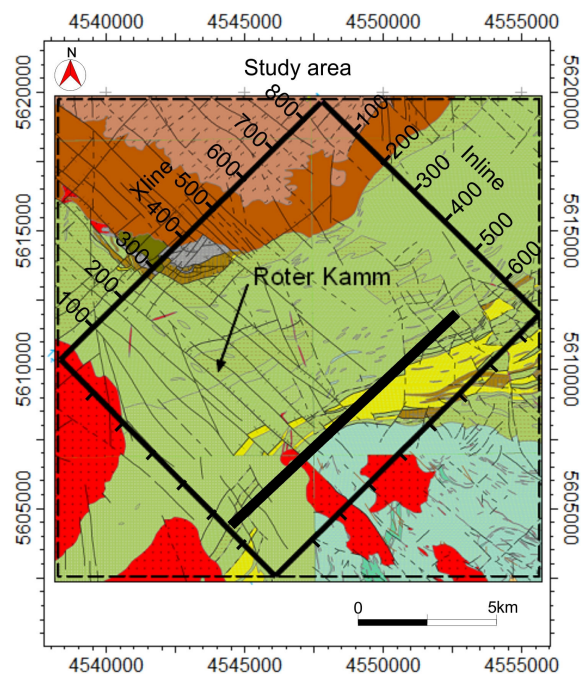


Figure 1: Map of the study area. The black box indicates the surface layout of the 3-D survey.

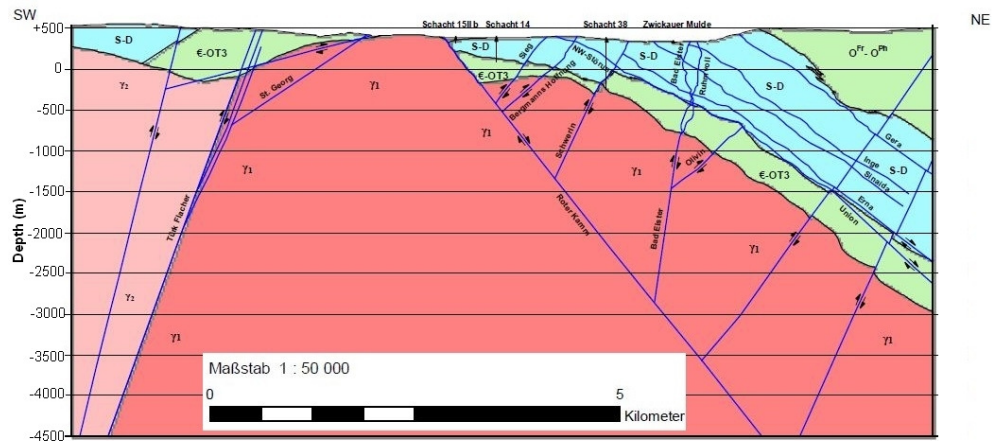


Figure 2: Geological cross section of the study area following the line in Figure 1

APPLICATION

The 3-D CRS processing was applied to the Schneeberg crystalline rock reflection data. The data have a very poor signal-to-noise ratio typical for hard rock environments. Figure 3 (a) shows the image of the brute stack for in-line 390 where the reflectivity of the transition zone from metamorphic to igneous is visible with little indication in the upper right part of the section. As expected, the image is very poor. Please note, that there are boundary effects in the very left and right parts of the section. Since the CMP stack did not provide a good image we had the hope that the CRS method can provide a better image. In Figure 3 (b) the CRS stacked section of the same line is shown (note again boundary effects). Reflectors here are clearer and more easy to distinguish in comparison to the brute stack. However, also the quality of the CRS stacked section is not really impressive despite the increased S/N ratio. Therefore we consider also the coherence as an image. It should display very similar features as the stack but with a decreased resolution since its value is always positive.

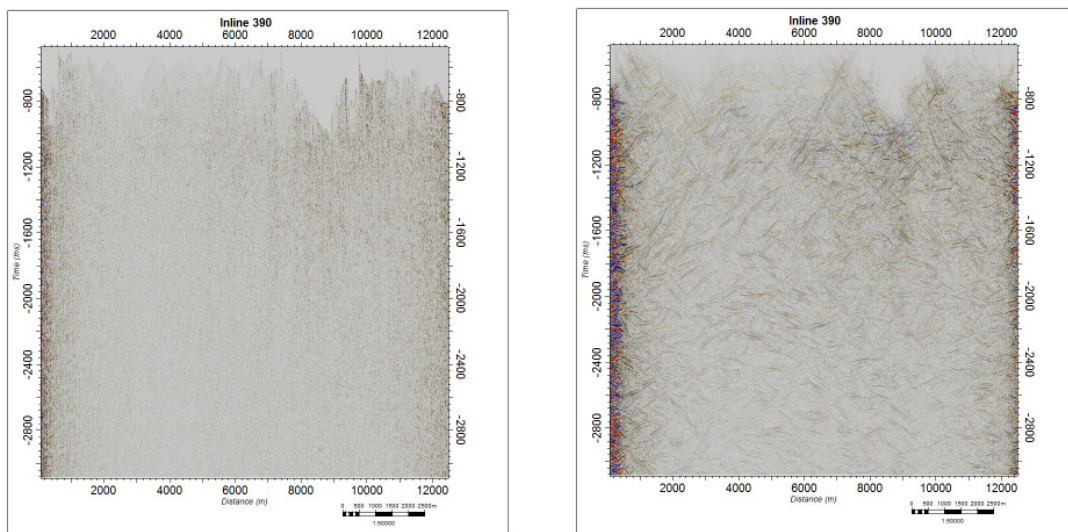


Figure 3: (a) 3D Brute Stack in-line 390 (left), (b) 3D CRS stack in-line 390 (right).

The coherence section for in-line 390 is displayed in Figure 4 (a). We observe scattered energy in the left part of the section not so well visible in the CRS stack. This could be an effect of the windowed normalization of the coherence evaluation equalizing the event amplitudes in the whole section. For data with very good S/N ratio a coherence section should be similar to a stacked section where absolute amplitudes are stacked. For noisy data, however, the coherence section is clearly superior to a stacked section with absolute amplitudes since it does enhance noise. The observed cluster of scattered energy in Figure 4 (a) may be related to an extended fracture zone. Whether the fractures are open or mineralized can not be concluded from the current state of processing. It should be noted that in the NW of the study area intensive mining was carried out. Here many of the found fracture systems were mineralized. The section in Figure 4 (a) also shows many events with a dip to the SW (i.e., right). These dips are associated with the conjugate faults intersecting the Rote Kamm almost perpendicularly. It is known from surface geology that many steep dipping events with dips to the SW and NE can be expected. The extend of such events observed in Figure 4 (a) is huge and may be also caused by many diffraction tails in the stack.

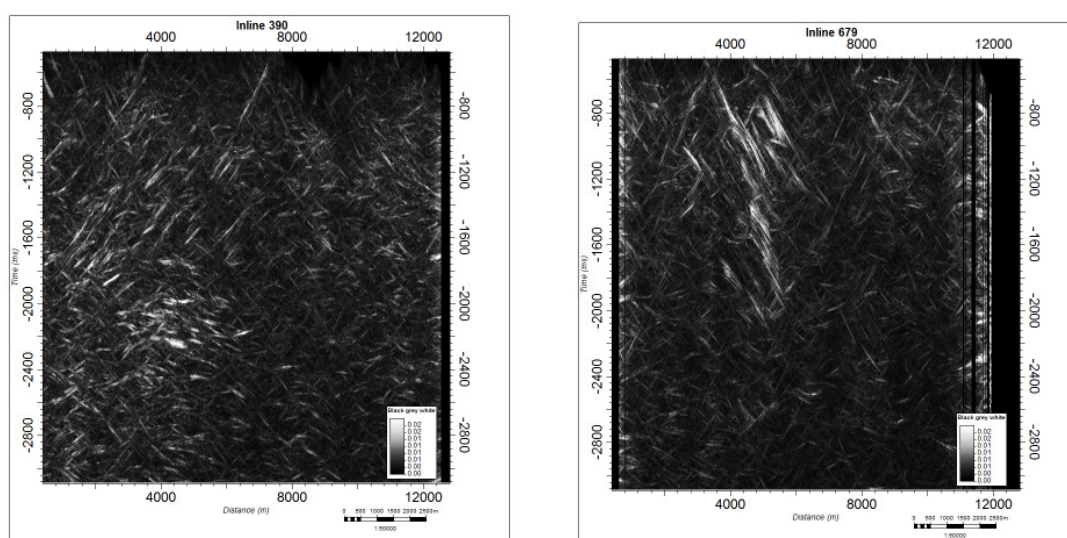


Figure 4: (a) 3D coherence sections of in-line 390 (left), (b) in-line 679 (right).

In Figure 4 (b) the coherence of a section close to SE boundary of the survey is displayed. This section shows very strong events dipping to the NE which we can attributed to the Roter Kamm system. A possible reason for the prominent occurrence of these events in this sections compared to in-line 390 may be given in the geological map. In Figure 1 we can identify an intrusive structure (red object) which is separated from the metamorphic rocks by the Rote Kamm fracture system. This could lead to a stronger impedance change when compared to the regions where the Rote Kamm intersects just metamorphic sequences. The direct comparison of CRS stacks and coherence sections has shown that the latter may provide more informations than the stack. For low S/N data from hard rock environments the coherence section may provide an alternative section valuable in the interpretation process. In the next paragraph we will now consider time slices out of a CRS stacked and coherence volume.

Figure 5 shows for time slices out of the CRS stack volume (right) and the coherence volume (left) for four different times. Please note the strong boundary effects in the results of the stacked volume. The figure somewhat repeats the experience of the previous images. The times slices from the stacked volume are very difficult to interpret. The information content of the time slices from the coherence volume is much smaller but distinct. We can clearly identify an area where most reflected energy is observed in the surface. This area is located in the southwestern part of the volume in about the middle of the survey box.

To further illustrate the findings of this section we have displayed 3-D images of the coherency cube which is cut at three different in-line positions (679,374, and 122, see Figure 6). Many steep events with

dips to the NE and SW are clearly visible. Because of steep structures and a lot of diffractions numerous conflicting dip situations are present. The NE and SW dipping events resemble the major fault systems of this area but may be partially also attributed to diffraction tails. The latter may intersect large parts of the stacked and coherence sections and can be collapsed, e.g., in a time migration. Stacks and coherence are entirely data driven processes and a result of just data fitting whereas the time migration represents an interpretation step since it requires a migration velocity. For the imaging of diffraction dominated data migration is essential. This is clearly illustrated by the previous results. In a first attempt we choose a constant migration velocity of 6 km/s and applied a post-stack Kirchhoff migration.

The time migrated sections of in-line 128 and 300 are displayed in Figure 7. Most steep dipping events are focused now indicating in fact that most of the dipping structures in the stacks and coherence belong to diffraction tails. However, a few steep events remain but are now much more focused to the geological features of the area. The time migrated section of in-line 128 clearly shows the Roter Kamm. It touches the surface at about 3500 m and is visible up to 2000 ms at 8000m horizontal position. It is the most extended event in the whole section which can be clearly correlated despite its broken structure. There is also some indication of conjugate faults in this section but they are much better visible in the time migrated section of in-line 300. A whole sequence of events dipping with about the same dips are observed in this image. Between 2000 and 5000 m at 2000 and 2800 ms we observe a zone of high reflectivity which comprises predominantly horizontal events. The geological reason of this zone is not yet resolved but could be important for the geothermal study if it is related to open fractures.

CONCLUSION

We have presented the application of the 3D CRS-based workflow to the Schneeberg 3-D hard rock reflection seismic data. The S/N ratio of these data is very low and neither the CMP nor the CRS-stacks did provide good images. The data are dominated by diffractions generated at various steep dipping fracture zones. Steep structures and a huge number of diffraction tails interfere or lead to a complicated pattern of conflicting dips. This makes the interpretation of the stacks very difficult. Displays of the coherence actually provided the best images, at least they showed a closer relation to the expected geology. Similar conclusions apply to the display of time slices where coherence slices provided the best images compared to time slices out of the stacked volume. The presence of large diffraction events in the data requires migration for the interpretation. We applied pre-stack Kirchhoff time migration using a constant velocity of 6 km/s. The obtained sections out of the migrated volume show the major geological features of the area, particular the steep dipping events of the Rote Kamm and a whole sequence of conjugate faults. The time migration of the coherency might provide an alternative approach not yet tested on these data. The greatest effort needs to be imposed on the improvement of the pre-stack data quality. Here the CRS method provides a suitable option through the partial stack facility.

OUTLOOK

Pre-stack time and depth migration will rely on the quality of the underlying velocities. Because of the poor data quality the estimation of CRS attributes is not necessarily stable and all processes relying on these attributes may be compromised. Key element in the processing of hard rock data is the enhancement of the pre-stack data quality. Partial stacks might be the best option to improve the image quality, however, if the attributes are poor, the enhancement result might not be effective. The data are largely dominated by diffractions which are not well fitted by the CRS operator. Processing the data with the i-CRS operator might improve the determination of wave field attributes since it better fits diffractions. High quality attributes will result in better time migration velocities, improved NIP wave tomography and better pre-stack data enhancement opportunities.

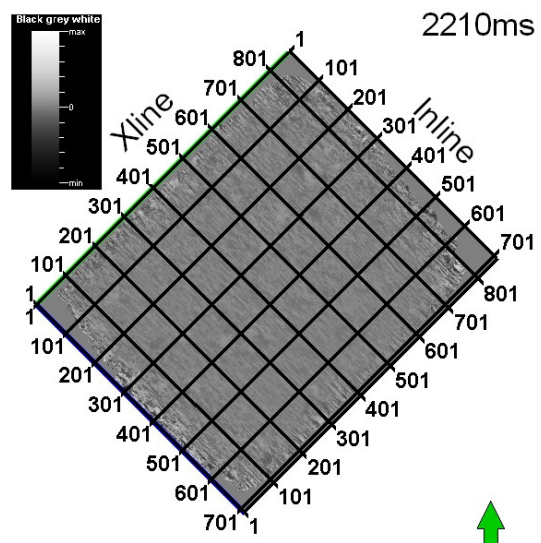
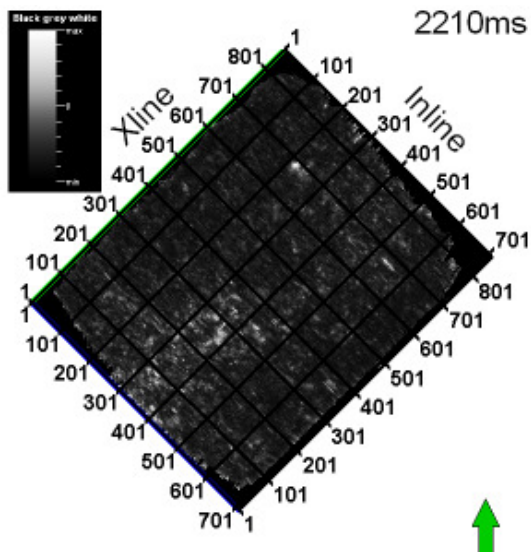
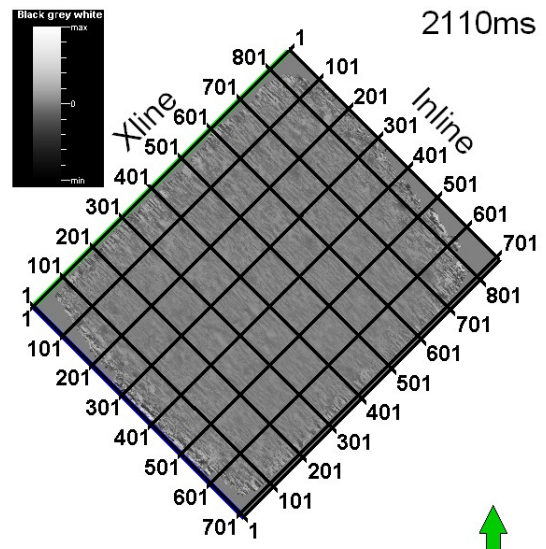
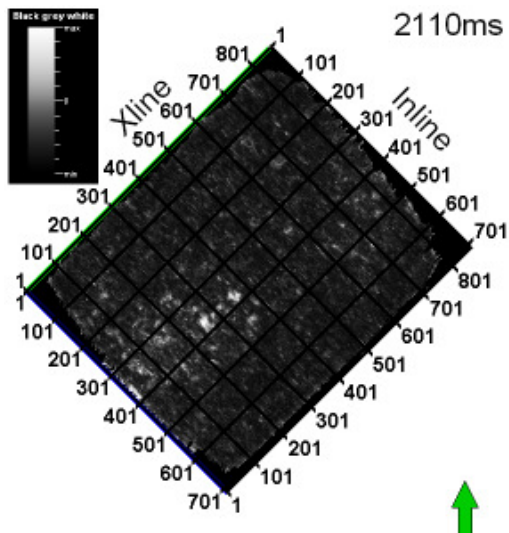
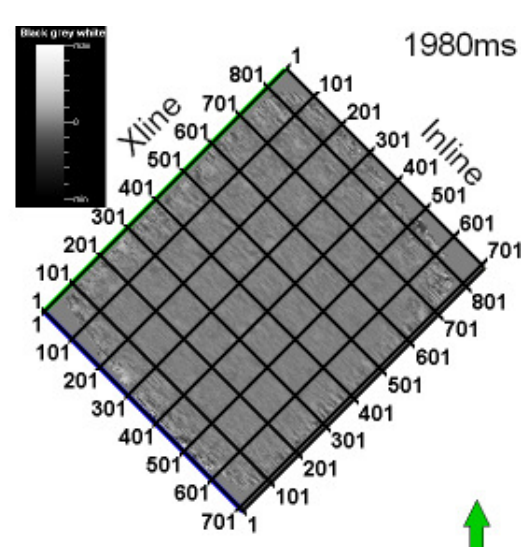
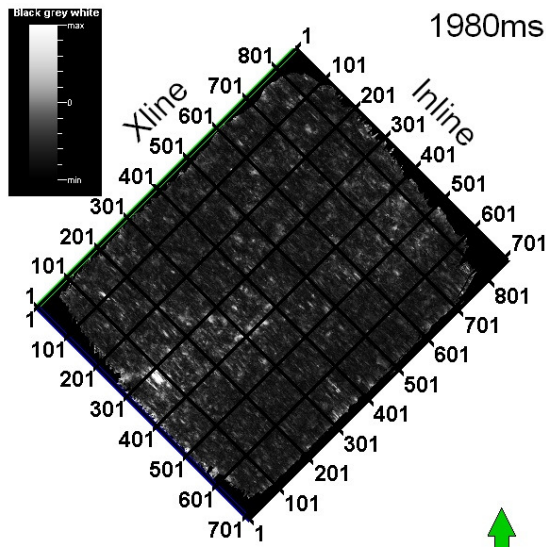
ACKNOWLEDGMENTS

This work was partially supported by the sponsors of the *Wave Inversion Technology (WIT) Consortium*. Special thanks for the BMU (Bundesministerium für Umwelt, Naturschutz und Reaktorsicherheit) German Ministry of Science and technology for providing the opportunity to work on this dataset. The discussions with the project partners of the University of Freiberg, Freiberg, Germany and, Leibniz Institute for Applied

Geophysics, Hannover, Germany, is highly appreciated. We would like to thank the Applied Geophysics Group Hamburg for continuous discussions.

REFERENCES

- Baykulov, M., Dümmonng, S., and Gajewski, D. (2011). From time to depth with CRS attributes. *Geophysics*, 76(4):S151–S155.
- Emmermann, R. and Wohlenberg, J. (1988). German Continental Deep Drilling Program(KTB). pages 39–40.
- Hertweck, T., Schleicher, J., and Mann, J. (2007). Data stacking beyond CMP. *The Leading Edge*, 26:818–827.
- Hubral, P. (1983). Computing true amplitude reflections in a laterally inhomogeneous earth. *Geophysics*, 48(8):1051–1062.
- Jäger, R., Mann, J., Höcht, G., and hubral, P. (2001). Common-reflection-surface stack: Image and attributes. *Geophysics*, 66(1):97–109.



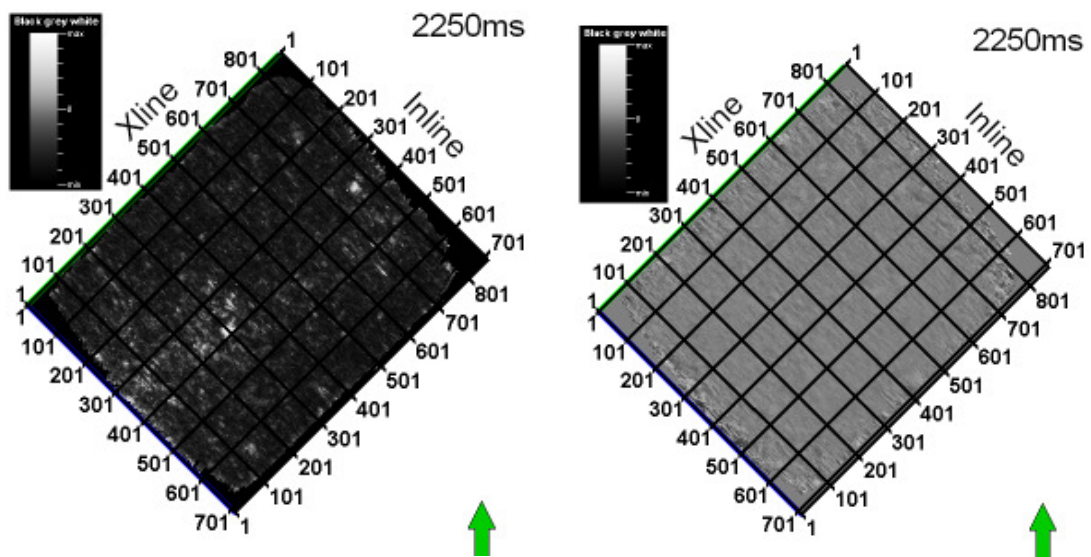
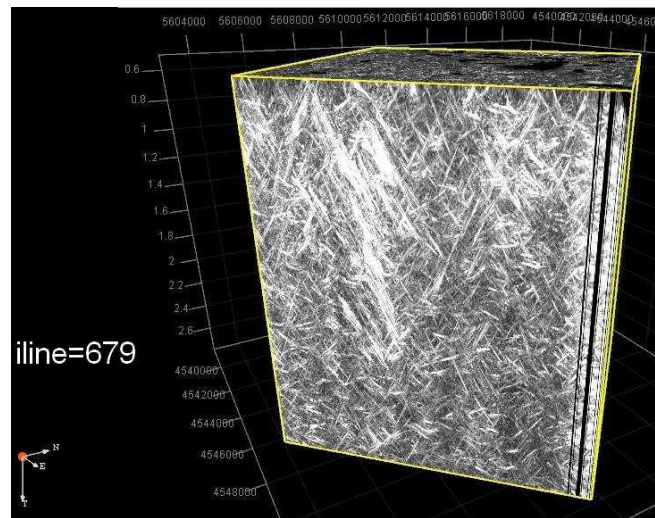
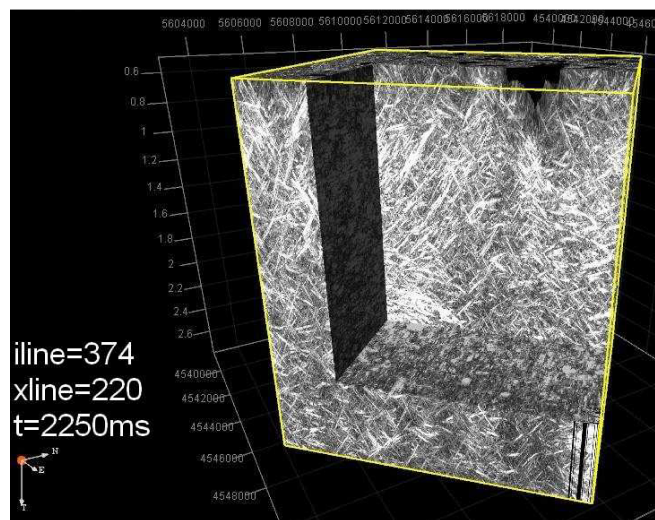


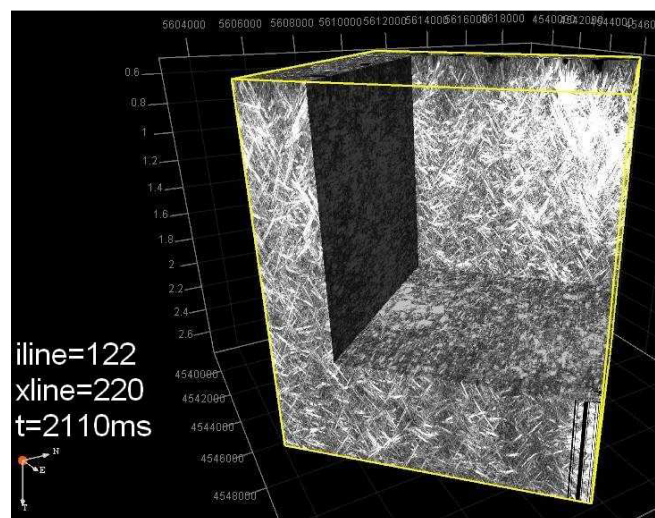
Figure 5: Time slices of coherence (left) and seismic cube (right).



(a)

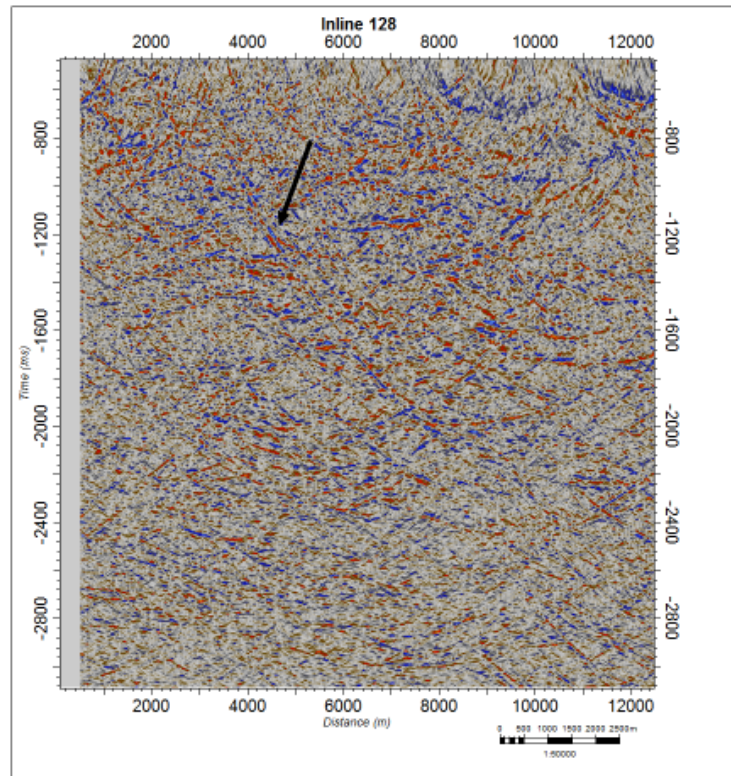


(b)

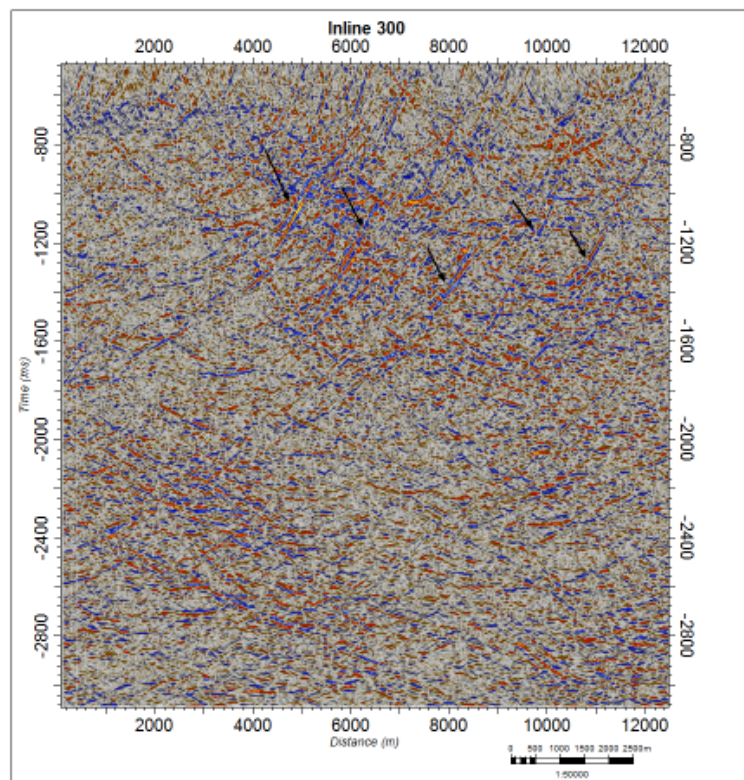


(c)

Figure 6: 3D CRS coherence cubes, (a) in-line 679, (b) in-line 374, (c) in-line 122



(a)



(b)

Figure 7: Kirchhoff post-stack time migrated sections of in-line 128 (a) and 300 (b). Roter Kamm and conjugate faults are indicated by arrows.